

---

# AFFINITY GUIDED GEOMETRIC SEMI-SUPERVISED METRIC LEARNING

---

A PREPRINT

Ujjal Kr Dutta, Mehrtash Harandi, and Chellu Chandra Sekhar

## ABSTRACT

In this paper, we address the semi-supervised metric learning problem, where we learn a distance metric using very few labeled examples, and additionally available unlabeled data. To address the limitations of existing semi-supervised approaches, we integrate some of the best practices across metric learning, to achieve the state-of-the-art in the semi-supervised setting. In particular, we make use of a graph-based approach to propagate the affinities or similarities among the limited labeled pairs to the unlabeled data. Considering the neighborhood of an example, we take into account the propagated affinities to mine triplet constraints. An angular loss is imposed on these triplets to learn a metric. Additionally, we impose orthogonality on the parameters of the learned embedding to avoid a model collapse. In contrast to existing approaches, we propose a stochastic approach that scales well to large-scale datasets. We outperform various semi-supervised metric learning approaches on a number of benchmark datasets.

**Keywords** Distance Metric Learning, Semi-Supervised Metric Learning, Graph-Based Learning, Riemannian Optimization.

## 1 Introduction

The Distance Metric Learning (DML) problem seeks to learn an embedding where similar examples are brought closer, while moving away dissimilar ones. Majority of the DML approaches require manual annotations or class labels to obtain constraints for optimizing the metric learning objective. In some applications, such as medical imaging techniques requiring invasive procedures, it may be possible to obtain only a limited amount of labeled data.

In this paper, we address the Semi-Supervised DML (SSDML) problem by learning a metric using only a limited amount of labeled data, and additionally available unlabeled data. An illustration of our method is present in Figure 1. Using a graph-based approach, we propagate the information from the labeled pairs to the unlabeled data. Considering the neighborhood of an example, we take into account the propagated similarities to mine triplet constraints. We impose an angular constraint on these triplets to learn a metric. Additionally, we impose orthogonality on the parameters of the learned embedding to avoid a model collapse.

Following are our major contributions: 1. We seamlessly integrate some of the best practices across metric learning, to achieve the state-of-the-art in the semi-supervised metric learning setting, 2. We propose a stochastic approach that scales well to large-scale datasets, and 3. We compare our method against some of the state-of-the-art semi-supervised DML methods, and empirically demonstrate that our method outperforms the baseline approaches on a number of benchmark datasets.

## 2 Related work

The Laplacian Regularized Metric Learning (LRML) [1] approach is a SSDML approach that employs the *min-max principle* to make use of the pairs of examples obtained from the limited labeled data. The min-max principle refers to minimizing the distance between the semantically similar pairs, while maximizing the distance between the dissimilar pairs. It captures the topology of the unlabeled data by virtue of a Laplacian regularizer [2] computed using a nearest neighbor graph. However, the weights of the graph are naively computed using the Euclidean distances in the original feature space, that itself may not be able to adequately represent the data.

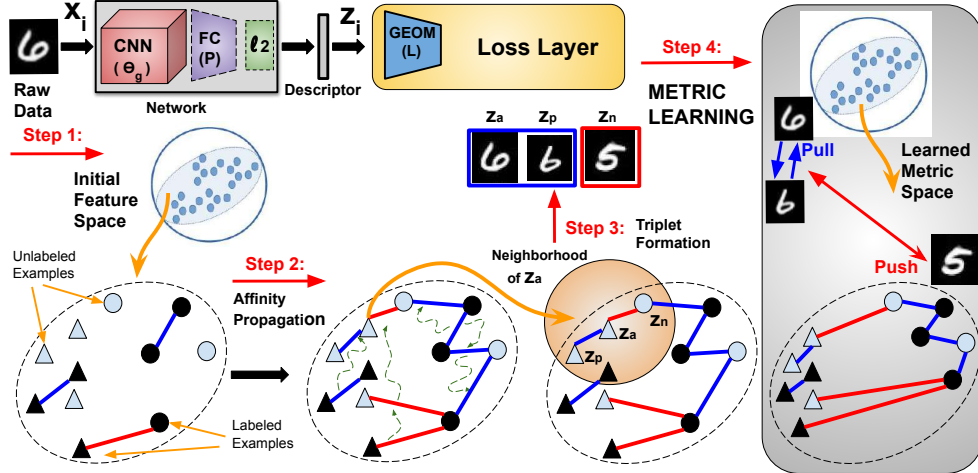


Figure 1: An illustration of our method (Best viewed in color). Examples of the same class are shown with similar shape.

The Affinity Propagation based Semi-Supervised Metric Learning (APSSML) framework [3] recently argued in favour of using a paradigm apart from the min-max principle to make use of the labeled pairs, by virtue of a prior metric computed using a supervised approach. Depending on whether a Log-Likelihood Ratio based prior metric is used, or an Information Theoretic prior metric is used, the APSSML framework yields two SSDML approaches, namely, the Affinity Propagation and Log-Likelihood Ratio (APLLR), and Affinity Propagation and Information-Theoretic (APIT) semi-supervised metric learning methods. However, when the labeled data is scarce, the prior metric computed using the supervised approach itself is poor in nature, and the resulting matrix is sometimes close to being singular.

The recently proposed state-of-the-art Intrinsic Steepest Descent based semi-supervised Metric Learning (ISDML) [4] approach makes use of an adaptive term to balance the influences of the inter-class and intra-class data samples obtained from labeled data. Due to the nature of the parameters of the objective, the authors employ a steepest descent approach on a Riemannian manifold. To utilize the unlabeled data, it uses a similar regularizer as the LRML method, based on a few assumptions for semi-supervised learning. However, this method is prone to suffer from a model collapse, where examples from different classes share a common embedding. This leads to a poor performance.

The Semi-supervised metRiC leArning Paradigm with Hyper-sparsity (SERAPH) [5] approach follows the *entropy minimization* principle [6] to make use of unlabeled data, along with the labeled constraints. *Entropy minimization* is known to ensure minimal overlap of classes, and hence leads to a good metric.

The classical *label propagation* approach by Zhou *et al.* [7], is a well-studied problem in the semi-supervised machine learning literature. However, the propagation of class labels to unlabeled data is too restrictive in nature. A rather flexible way of information spreading was that of *affinity propagation*, first discussed by Liu *et al.* [8]. The approach discussed therein learns a sparse metric by making use of a log-determinant term in conjunction to an adapted Laplacian regularizer used to facilitate affinity propagation. The affinity propagation principle forms the basis of the APLLr and APIT methods discussed above, and also our proposed method in this paper. The intuition of the affinity propagation principle is to propagate the similarities among the labeled pairs to the unlabeled ones. This is done by a random walk process on a nearest neighbor based graph.

### 3 The Problem

Let  $\mathcal{X} = \mathcal{X}_L \cup \mathcal{X}_U$  be a given dataset, consisting of a set of labeled examples  $\mathcal{X}_L = \{\mathbf{x}_i\}_{i=1}^{N_L}$  with the associated label set  $\{y_i\}_{i=1}^{N_L}$ , ( $y_i \in \{1, \dots, C\}$ ), and a set of unlabeled examples  $\mathcal{X}_U = \{\mathbf{x}_j\}_{j=N_L+1}^N$ . Here,  $C$  is the number of classes present in the training data. Assume that we have a function  $z : \mathcal{X} \rightarrow \mathbb{R}^d$  (say, a deep neural network) with parameters  $\theta_z$ , that provides a nonlinear embedding  $z_i \in \mathbb{R}^d$  for an example  $\mathbf{x}_i$ . Following are **our two major objectives**: 1. **Identify a set of triplets** of examples from  $\mathcal{X}$ , such that each triplet is of the form  $(z_i, z_i^+, z_i^-)$ . Here,  $z_i, z_i^+$  and  $z_i^-$  are called as the anchor, positive and negative respectively. The first two are supposed to be *semantically similar*, while the third being dissimilar to both. In the semi-supervised case, we propose to first propagate the affinities between pairs of examples from  $\mathcal{X}_L$ , to all the pairs in  $\mathcal{X}_L \cup \mathcal{X}_U$ . The propagated affinities are used to identify triplets. 2. Having identified a set of triplets, our goal is to learn the parameters  $\theta_z$  of the function  $z : \mathcal{X} \rightarrow \mathbb{R}^d$  in such a way that  $z_i$  and  $z_i^+$  are brought closer while pushing away  $z_i^-$  from them in the learned embedding. Essentially, we are **learning a**

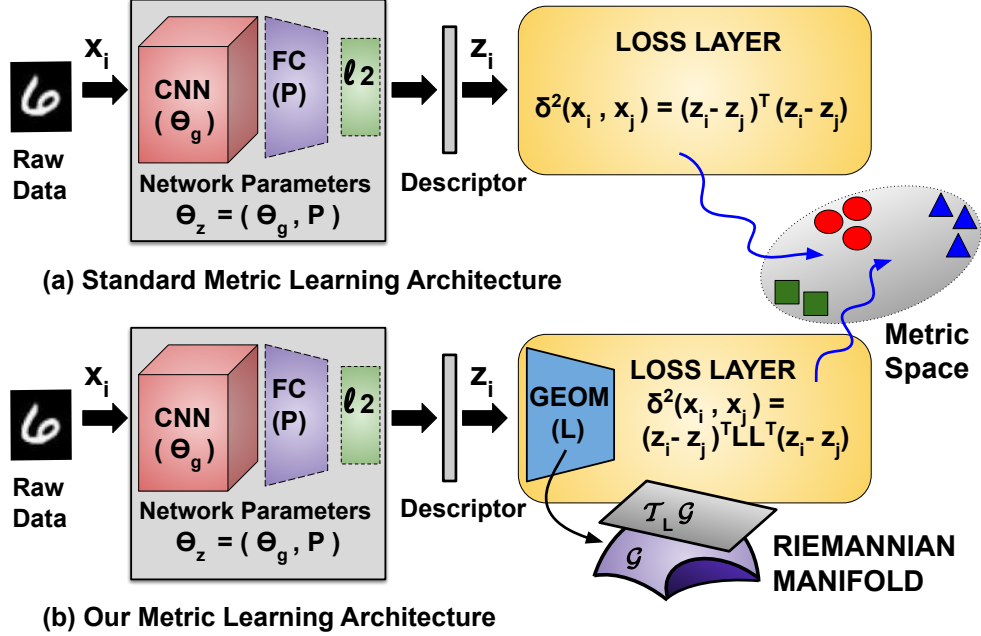


Figure 2: Comparison of our proposed architecture against standard metric learning architecture.

**distance metric function**  $\delta^2(\mathbf{x}_i, \mathbf{x}_j) = (\mathbf{z}_i - \mathbf{z}_j)^\top (\mathbf{z}_i - \mathbf{z}_j)$  such that distance between similar examples is smaller than that between two dissimilar ones.

## 4 Geometric aspect of our method

Essentially, one can subdivide the parameter set as:  $\theta_z = (\theta_g, \mathbf{P})$ , where  $\mathbf{P}$  is the parametric matrix of a Fully-Connected (FC) layer at the end, and  $\theta_g$  consists of the parameters of the remaining network (Figure 2-a). Existing supervised DML approaches [9, 10] jointly learn the parameters  $(\theta_g, \mathbf{P})$  using a set of constraints obtained using the class label set  $\{y_i\}$ . These constraints can be in the form of triplets  $(z_i, z_i^+, z_i^-)$ , as discussed above. The idea is to learn  $\delta^2(\mathbf{x}_i, \mathbf{x}_i)$  by bringing  $z_i$  and  $z_i^+$  closer, while moving away  $z_i^-$  from the other two.

Xie *et al.* [11] recently cited the following reasons for imposing a geometric constraint in the form of orthogonality, on the metric parameters: 1. When we have limited labeled data, overfitting may occur, 2. In case of class imbalance, the frequent classes may influence the metric learning [11] to their favour, and 3. By learning a compact set of projection vectors, it reduces redundancy in the learned metric. Also, mining arbitrarily hard triplets may put the model at the risk of a collapse [12], where we get degenerate poor embeddings. Recent studies in deep learning [13–15], and metric learning [11, 16–19], also have shown the benefits of imposing orthogonality. Orthogonality also leads to empirical performance improvement, and a stable training [14].

However, a direct imposition of orthogonality on the FC layer, *i.e.*, on  $\mathbf{P}$ , requires non-trivial Riemannian extensions of SGD [20], thus not making it readily applicable to standard SGD in deep learning. This is because SGD cannot preserve constraints during weight update. Hence, we propose a crafty modification to the standard architecture, wherein we introduce an *orthogonal matrix*  $\mathbf{L} \in \mathbb{R}^{d \times l}$ ,  $l \leq d$  ( $\mathbf{L}^\top \mathbf{L} = \mathbf{I}_l$ ) resembling a GEOMETRIC (GEOM) sublayer *within* the metric learning loss layer itself (see Figure 2-b). Thus, the distance function can now be expressed as:  $\delta^2(\mathbf{x}_i, \mathbf{x}_j) = (\mathbf{z}_i - \mathbf{z}_j)^\top \mathbf{L} \mathbf{L}^\top (\mathbf{z}_i - \mathbf{z}_j)$ .  $l < d$  can facilitate dimensionality reduction, thus enabling us to efficiently handle high-dimensional data.

Consider the orthogonal group  $\mathcal{O}(l) = \{\mathbf{B} \in \mathbb{R}^{l \times l} : \mathbf{B} \mathbf{B}^\top = \mathbf{B}^\top \mathbf{B} = \mathbf{I}_l\}$ . It should be observed that for a matrix  $\mathbf{B} \in \mathcal{O}(l)$ , and any objective function  $\mathcal{L}(\mathbf{L})$  involving  $\delta^2(\mathbf{x}_i, \mathbf{x}_i)$ , replacing  $\mathbf{L}$  in  $\delta^2(\mathbf{x}_i, \mathbf{x}_i)$  by  $\mathbf{L} \mathbf{B}$  does not change the value of the objective, since  $(\mathbf{L} \mathbf{B})(\mathbf{L} \mathbf{B})^\top = \mathbf{L} \mathbf{L}^\top$ , *i.e.*,  $\mathcal{L}(\mathbf{L}) = \mathcal{L}(\mathbf{L} \mathbf{B})$ . From a Riemannian geometric perspective [21], we say that the objective is invariant to the right action of the group  $\mathcal{O}(l)$ . This could be detrimental to the performance of the optimization method. Hence, the correct geometry to consider for  $\mathbf{L}$  is that of the Grassmann manifold  $\mathcal{G}(l, d)$  [21] (details in supplementary).

## 5 The stochastic semi-supervised aspect using affinities

Having decided the proper geometric structure for  $L$ , and the necessary changes in the architecture, we now discuss the aspect of triplet mining for our semi-supervised approach. Let  $\mathcal{X}_U^{(p)}$  be a randomly selected partition of unlabeled data. We consider it along with the labeled data  $\mathcal{X}_L$  to learn a metric. Using  $\mathcal{X}_L \cup \mathcal{X}_U^{(p)}$ , we construct a nearest neighbour graph such that the nodes represent the examples, with edges between nearest neighbors. The edge weights denote the *affinities* (or similarities) among the examples. Note that to construct the graph, we make use of the  $l_2$ -normalized embeddings  $\{z_i\}$  such that  $z_i = z(\mathbf{x}_i; \theta_z)$ , and  $\mathbf{x}_i \in \mathcal{X}_L \cup \mathcal{X}_U^{(p)}$ .

Let,  $N_L$  and  $N_p$  be the respective cardinalities of the sets  $\mathcal{X}_L$  and  $\mathcal{X}_U^{(p)}$ . We define an initial affinity matrix  $\mathbf{W}^0 \in \mathbb{R}^{(N_L+N_p) \times (N_L+N_p)}$  as follows:

$$W_{ij}^0 = \begin{cases} +1 & , \text{if } i \neq j \text{ and } \exists y_i, y_j, \text{ s.t. } y_i = y_j, \\ -1 & , \text{if } i \neq j \text{ and } \exists y_i, y_j, \text{ s.t. } y_i \neq y_j, \\ +1 & , \text{if } i = j, \\ 0 & , \text{otherwise.} \end{cases} \quad (1)$$

Here, we assign an affinity (similarity) of +1 for pairs of examples belonging to the same class and an affinity of  $-1$  for pairs of examples belonging to different classes. The self affinities are set as +1, and we also ensure that  $\mathbf{W}^0$  is symmetric. Our goal is to ensure the flow of information from the non-zero entries of  $\mathbf{W}^0$  (representing the labeled pairs) to the zero entries representing the unlabeled pairs. To do so, we follow the affinity propagation principle [8], by constructing the neighborhood indicator matrix  $\mathbf{Q} \in \mathbb{R}^{(N_L+N_p) \times (N_L+N_p)}$  defined as follows:

$$N_{ij} = \begin{cases} 1/k & , \text{if } z_j \in \mathcal{N}_k(z_i), \\ 0 & , \text{otherwise.} \end{cases} \quad (2)$$

Here,  $\mathcal{N}_k(z_i)$  is the set of  $k$ -nearest neighbor examples of  $z_i$ .  $\mathbf{Q}$  is asymmetric in nature. By using the neighborhood structure indicated by  $\mathbf{Q}$ , we can propagate the affinities among the labeled pairs to the unlabeled ones by performing a step described by Liu *et al.* [8], as follows:

$$\mathbf{W}^* = (1 - \gamma)(\mathbf{I}_{N_L+N_p} - \gamma\mathbf{Q})^{-1}\mathbf{W}^0. \quad (3)$$

Here, (3) essentially performs a Markov random walk step, and  $0 < \gamma < 1$  is a weight parameter to provide a trade-off between the affinity matrix obtained at a step, with that of the initial one, *i.e.*,  $\mathbf{W}^0$ . As  $N_L + N_p \ll N$ , we do not encounter any difficulty while scaling up to large datasets. To obtain a symmetric affinity matrix  $\mathbf{W}$ , we perform a final symmetrization step as follows:  $W_{ij} = (W_{ij}^* + W_{ji}^*)/2$ .

### 5.1 Mining triplets using propagated affinities

The finally obtained representation of the symmetric affinity matrix  $\mathbf{W}$  is used to mine triplets for metric learning. In doing so, we take into account the  $k$ -neighborhood  $\mathcal{N}_k(z_a)$  of an example  $z_a \in \mathcal{X}_L \cup \mathcal{X}_U^{(p)}$  that we consider as an anchor. Let  $\mathcal{N}_W(z_a) = \{z_1^+, z_2^+, \dots, z_{k/2}^+, z_{k/2+1}^-, z_{k/2+2}^-, \dots, z_k^-\}$  be the  $k$ -neighboring examples of  $z_a$  sorted in descending order of their *propagated affinities* w.r.t.  $z_a$ , *i.e.*,  $\mathbf{W}(z_a, z_1^+) > \dots > \mathbf{W}(z_a, z_{k/2}^+) > \mathbf{W}(z_a, z_{k/2+1}^-) > \dots > \mathbf{W}(z_a, z_k^-)$ . Essentially,  $\mathcal{N}_W(z_a)$  is simply a sorted version of  $\mathcal{N}_k(z_a)$ . As the obtained affinities are an indication of the semantic similarities among examples, we take it as a guidance to form triplets. Given an anchor  $z_a$ , intuitively we can consider an example  $z_i^+$  with more affinity towards  $z_a$  as a *positive*, and another example  $z_j^-$  with lesser affinity towards  $z_a$  as a *negative*, and form a triplet  $(z_a, z_i^+, z_j^-)$ . By considering first half of examples in the sorted neighborhood  $\mathcal{N}_W(z_a)$  as *positives*, and remaining half as *negatives*, we can form the following triplets:  $(z_a, z_1^+, z_{k/2+1}^-), (z_a, z_2^+, z_{k/2+2}^-), \dots, (z_a, z_{k/2}^+, z_k^-)$ . One may select the set of anchors from entire  $\mathcal{X}_L \cup \mathcal{X}_U^{(p)}$ , or by seeking the modes of the graph, without loss of generality. Figure 3 shows an illustration of this idea with  $k = 4$ .

### 5.2 Metric learning using triplets

Given  $\mathcal{X}_L \cup \mathcal{X}_U^{(p)}$  and the corresponding  $\mathbf{W}$ , assume that we have obtained a triplet set  $\mathcal{T}_p = \bigcup_b \mathcal{T}_p^{(b)}$ . Here,  $\mathcal{T}_p^{(b)}$  is a mini-batch of  $T_b$  triplets, and  $b \in [1, \dots, \lfloor \frac{|\mathcal{T}_p|}{T_b} \rfloor]$ . Let,  $\mathcal{T}_p^{(b)} = \{(z_i, z_i^+, z_i^-)\}_{i=1}^{T_b}$ . Then, we can learn the parametric matrix  $L$  by minimizing the following objective:

$$J_{metric} = \sum_{i=1}^{T_b} \log(1 + \exp(m_i)), \quad (4)$$

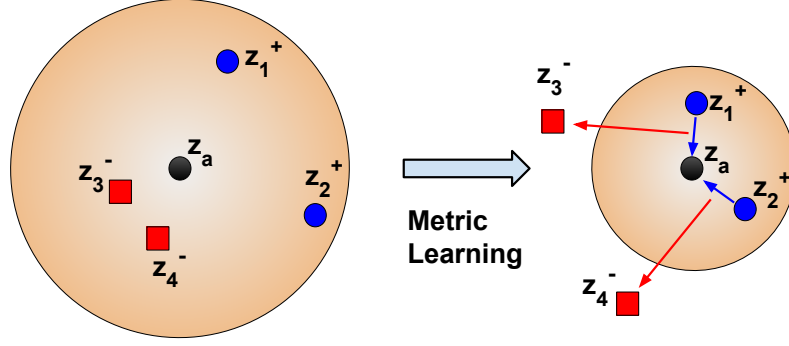


Figure 3: Neighborhood triplet mining using propagated affinities (best viewed in color).  $z_a, z_1^+, z_2^+, z_3^-, z_4^- \in \mathcal{X}_L \cup \mathcal{X}_U^{(p)}$ . An anchor  $z_a$  (shown in black) is a point in the dataset that is currently in consideration for triplet mining within its  $k$ - neighborhood  $\mathcal{N}_k(z_a)$ ,  $k=4$  (based on Euclidean distances in current embedding space). Points in blue ( $z_1^+, z_2^+$ ) are more *semantically* similar (by virtue of *propagated affinities*) to the anchor, than the points in red ( $z_3^-, z_4^-$ ). In the current embedding, the blue points are farther from the anchor  $z_a$  than the red ones, despite having more semantic similarity. Hence, they should be pulled closer to the anchor in the learned space, compared to the red ones. In short, as  $z_1^+, z_2^+, z_3^-, z_4^- \in \mathcal{N}_k(z_a)$ , s.t.,  $\mathbf{W}(z_a, z_1^+) > \mathbf{W}(z_a, z_2^+) > \mathbf{W}(z_a, z_3^-) > \mathbf{W}(z_a, z_4^-)$ , we form the following triplets:  $(z_a, z_1^+, z_3^-)$  and  $(z_a, z_2^+, z_4^-)$ .

such that

$$m_i = \delta_{\mathbf{L}}^2(z_i, z_i^+) - 4 \tan^2 \alpha \delta_{\mathbf{L}}^2(z_i^-, z_{i-avg}). \quad (5)$$

Here,  $z_{i-avg} = (z_i + z_i^+)/2$ , and  $\delta_{\mathbf{L}}^2(z_i, z_j) = (z_i - z_j)^\top \mathbf{L} \mathbf{L}^\top (z_i - z_j)$ . The objective in (4) is a *smooth* angular loss [10] that tries to pull the anchor  $z_i$  and the positive  $z_i^+$  together, while moving away the negative  $z_i^-$  from the mean  $z_{i-avg}$  with respect to an angle  $\alpha > 0$  which is a hyperparameter. Given the fact that  $J_{metric}$  in (4) is fully-differentiable, we can backpropagate the gradients to learn the parameters  $\theta_z$  of the nonlinear embedding. Hence, the overall optimization problem of our metric learning approach can be expressed as:

$$\min_{\mathbf{L} \in \mathcal{G}(l, d), \theta_z} J_{metric}. \quad (6)$$

Usually, after each Euclidean gradient update step, the orthogonality is lost. Hence, for each mini-batch of triplets  $\mathcal{T}_p^{(b)}$ , we perform Riemannian optimization to learn the parametric matrix  $\mathbf{L}$  while maintaining the constraint  $\mathbf{L} \in \mathcal{G}(l, d)$  (more details in supplementary). We call our proposed approach in (6) as **Affinity guided Geometric semi-supervised Metric Learning (AGML)**, and describe it in Algorithm 1.

---

**Algorithm 1** Our stochastic approach

---

**Input:** Data set  $\mathcal{X} = \mathcal{X}_L \cup \mathcal{X}_U = \{\mathbf{x}_i\}_{i=1}^{N_L} \cup \{\mathbf{x}_j\}_{j=N_L+1}^N, \{y_i\}_{i=1}^{N_L}$ , with  $N_L \ll N$ . Backbone network  $z : \mathcal{X} \rightarrow \mathbb{R}^d$  s.t.  $z_k = z(\mathbf{x}_k; \theta_z), \forall \mathbf{x}_k \in \mathcal{X}$ .

- 1: Initialize  $\theta_z, \mathbf{L}_{prev}$ .
- 2: **for**  $count \leftarrow 1$  to  $maxcount$  **do**
- 3: Randomly sample partition  $\mathcal{X}_U^{(p)}$  s.t.  $|\mathcal{X}_U^{(p)}|$  is sufficiently large enough (say  $|\mathcal{X}_U^{(p)}| \approx 9N_L, |\mathcal{X}_U^{(p)}| < N - N_L$ ).
- 4: Obtain current representation  $z(\mathcal{X}_L) \cup z(\mathcal{X}_U^{(p)})$ .
- 5: ▷ STEP 1 of Figure 1
- 6: Perform Affinity propagation on the sub-graph corresponding to  $z(\mathcal{X}_L) \cup z(\mathcal{X}_U^{(p)})$ , to obtain the affinity matrix  $\mathbf{W}$ .
- 7: ▷ STEP 2 of Figure 1
- 8: Obtain  $\mathcal{T}_p = \bigcup_b \mathcal{T}_p^{(b)}$  using  $\mathbf{W}$ . ▷ STEP 3 of Figure 1
- 9: **for**  $epoch \leftarrow 1$  to  $maxepoch$  **do**
- 10: **for**  $b \in [1, \dots, \lfloor \frac{T_p}{T_b} \rfloor]$  **do** ▷ Performing AGML using  $\mathcal{T}_p^{(b)}$ .
- 11:  $[\mathbf{L}] \leftarrow \text{AGML}(\mathbf{L}_{prev})$ . ▷ STEP 4 of Figure 1
- 12:  $\mathbf{L}_{prev} = \mathbf{L}$ ;
- 13: Back-propagate to update  $\theta_z$ .
- 14: **end for** ▷ End of mini-batch for loop.
- 15: **end for**
- 16: **end for** ▷ End of count for loop.
- 17: **return**  $\theta_z, \mathbf{L}$

---

In the supplementary material, we provide an efficient algorithm for AGML. Our algorithm is linear in terms of the number of triplets in a mini-batch, *i.e.*,  $T_b$ , which is usually low. Also, the complexity of our algorithm is either



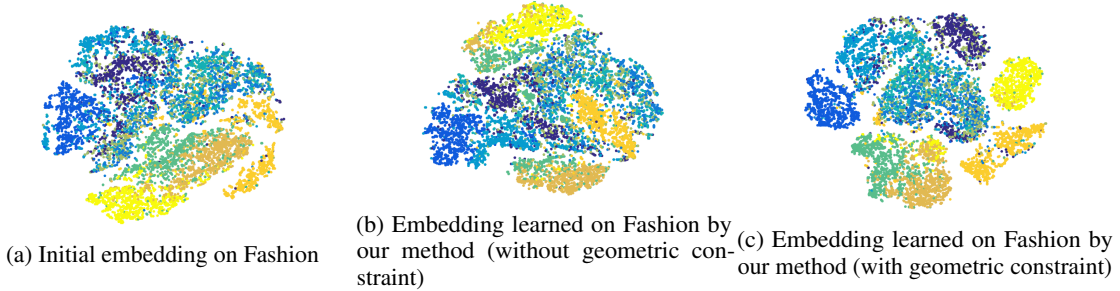


Figure 4: Qualitative evaluation of t-SNE embeddings obtained in various scenarios (Best viewed in color).

Table 1: Comparison against state-of-the-art semi-supervised metric learning approaches on MNIST, Fashion-MNIST and CIFAR-10.

Dataset	MNIST					Fashion-MNIST					CIFAR-10				
	NMI	R@1	R@2	R@4	R@8	NMI	R@1	R@2	R@4	R@8	NMI	R@1	R@2	R@4	R@8
LRML [1]	<b>48.3</b>	88.7	93.2	95.9	97.6	<b>53.2</b>	75.3	83.9	90.2	95.0	16.0	40.2	56.3	71.5	83.7
SERAPH [5]	45.3	92.5	95.7	97.6	98.7	53.0	75.9	85.1	91.5	95.4	21.3	39.5	56.2	71.1	83.7
ISDML [4]	44.1	92.1	95.7	97.5	98.6	51.3	74.4	84.2	90.7	95.1	20.0	36.4	52.4	68.5	82.1
APLLR [3]	30.5	57.6	71.1	82.1	90.1	38.9	59.5	73.3	84.1	91.4	13.3	24.4	40.0	58.8	76.4
APIT [3]	31.7	87.6	92.9	96.0	97.9	37.3	69.4	80.1	88.5	94.1	11.4	26.0	41.4	59.6	76.4
<b>AGML (Ours)</b>	47.5	<b>93.9</b>	<b>96.6</b>	<b>98.2</b>	<b>98.9</b>	52.1	<b>77.6</b>	<b>86.0</b>	<b>91.8</b>	<b>95.6</b>	<b>25.3</b>	<b>41.4</b>	<b>57.3</b>	<b>72.6</b>	<b>84.9</b>

linear or quadratic in terms of the original dimensionality  $d$ . Hence, AGML can effectively and efficiently handle high-dimensional data, in contrast to contemporary semi-supervised metric learning approaches that require  $O(d^3)$  complexity [1, 3].

## 6 Experimental Studies

In this section, we empirically evaluate our proposed method by comparing against important semi-supervised metric learning methods. In all experiments, the parameters of an embedding are learned using an approach on the training data, and the test examples are projected using the same. In the learned space, clustering and retrieval tasks are performed on the test embeddings. The Normalized Mutual Information (NMI) metric is used for evaluation of the clustering performance. It is defined as the ratio of mutual information and the average entropy of clusters and entropy of actual ground truth class labels. For evaluation in the retrieval task, the Recall@K (R@K) metric has been used. It gives us the percentage of test examples that have at least one K nearest neighbor from the same class. We first use the following datasets: MNIST [22], Fashion-MNIST [23], and CIFAR-10 [24]. The standard training and test splits have been used for all datasets.

We adapted the network architectures for MNIST and CIFAR-10 datasets in the MatConvNet tool [25]. For MNIST and Fashion datasets, the network for MNIST has been adapted as: Conv1( $5 \times 5, 20$ )  $\rightarrow$  max-pool  $\rightarrow$  Conv2( $5 \times 5, 50$ )  $\rightarrow$  max-pool  $\rightarrow$  Conv3( $4 \times 4, 500$ )  $\rightarrow$  ReLU  $\rightarrow$  FC( $500 \times 128$ )  $\rightarrow$   $l_2$   $\rightarrow$  GEOM( $128 \times 64$ ). For CIFAR-10, we used the following adapted network: Conv1( $5 \times 5, 32$ )  $\rightarrow$  max-pool  $\rightarrow$  ReLU  $\rightarrow$  Conv2( $5 \times 5, 32$ )  $\rightarrow$  ReLU  $\rightarrow$  avg-pool  $\rightarrow$  Conv3( $5 \times 5, 64$ )  $\rightarrow$  ReLU  $\rightarrow$  avg-pool  $\rightarrow$  Conv4( $4 \times 4, 64$ )  $\rightarrow$  ReLU  $\rightarrow$   $l_2$   $\rightarrow$  GEOM( $64 \times 32$ ).

For our AGML method,  $\gamma = 0.99$  in (3),  $k = 10$  in (2),  $\alpha = 40^\circ$  in (5), initial learning rate is  $10^{-3}$ . We run for a maximum of 50 epochs and choose the best model. Our model enjoys robustness to the choice of  $\alpha$  (in the range  $\alpha = 30^\circ$ - $60^\circ$ ), an observation similar to Wang *et al.* [10]. For MNIST and Fashion datasets, we choose 100 labeled examples (10 per class), while for CIFAR-10, we choose 1000 labeled examples (100 per class). For MNIST and Fashion, we fine-tune randomly initialized networks. For CIFAR-10, we pretrain with labeled examples (by replacing the GEOM with softmax) for 30 epochs, and then fine-tune using our AGML loss.

To justify our design choice of imposing orthogonality, we plot the tSNE embeddings of the test split of the Fashion dataset, obtained in various scenarios (see Figure 4). As per our conjecture, without orthogonality, there may be a model collapse, leading to degenerate clusters. By imposing orthogonality, we could observe well-separated, compact clusters. We discuss further ablation studies of our method in terms of empirical measures, along with tSNE embeddings for the other two datasets in the supplementary.

### 6.1 Comparison against state-of-the-art

In Table 1, we compare our method against the following state-of-the-art, semi-supervised metric learning approaches discussed in detail in Section 2: LRML [1], SERAPH [5], ISDML [4], APLLR [3] and APIT [3]. For the MNIST and Fashion datasets, the LRML approach works well for the clustering task. However, for the complex CIFAR-10, LRML

performed much worse than ours. The SERAPH method relying on entropy regularization does consistently well across all datasets.

The APLLR [3] and APIT [3] methods, that also make use of affinity propagation [8] as ours, could not outperform our method. This is because their tendency to restrict the learned metric to be close to a prior metric works well only when labeled data itself is sufficient. But when labeled data is extremely scarce, their labeled data based prior metric suffers severe overfitting, leading to a poor prior. Especially, the log-likelihood ratio based prior metric in APLLR results in scatter matrices which are near singular, leading to non-invertibility. However, our method on the other hand, harnesses the full potential of affinity propagation, by further mining informative triplets. Our method is nearly robust to the data distribution, as witnessed by its competitive performance in CIFAR-10, in contrast to the baselines.

Table 2: Comparison on fine-grained datasets.

Dataset	CUB-200 [26]					Cars-196 [27]				
Method	NMI	R@1	R@2	R@4	R@8	NMI	R@1	R@2	R@4	R@8
Initial	34.3	31.7	42.2	55.4	67.9	23.7	24.2	32.8	43.4	54.9
LRML [1]	49.9	34.9	45.0	55.4	65.7	40.5	33.2	41.2	49.4	58.3
SERAPH [5]	50.5	39.7	52.2	64.4	76.5	37.2	34.8	46.7	59.4	71.7
ISDML [4]	50.6	43.7	55.7	67.6	78.4	25.8	30.6	40.8	52.2	63.2
APLLR [3]	38.9	25.7	36.6	48.7	61.9	33.2	33.0	43.6	55.6	67.9
APIT [3]	52.1	42.2	54.5	66.7	78.2	37.3	38.5	50.7	62.7	74.9
<b>AGML (Ours)</b>	<b>54.0</b>	<b>44.8</b>	<b>56.9</b>	<b>69.1</b>	<b>79.9</b>	<b>40.7</b>	<b>45.7</b>	<b>58.1</b>	<b>69.5</b>	<b>80.4</b>

## 6.2 Comparison on fine-grained datasets

We also evaluate the methods on two benchmark Fine-Grained Visual Categorization (FGVC) datasets, namely, CUB-200 [26] and Cars-196 [27]. The **Caltech-UCSD Birds 200 (CUB-200)** [26] dataset consists of images of birds belonging to 200 species. The **Cars-196** [27] dataset consists of images of cars belonging to 196 models. We used the following standard evaluation protocol [9]: For CUB dataset, the first 100 species containing 5864 images are used for training, and the remaining 100 species containing 5924 images are used for testing. For Cars dataset, the first 98 models containing 8054 images are used for training, while the remaining 98 models containing 8131 images are used for testing. As test and training classes are disjoint, it corresponds to a Zero-Shot Learning (ZSL) setting.

The GoogLeNet [28] architecture pretrained on ImageNet [29], has been used as the backbone CNN, using the MatConvNet [25] tool. We used the Regional Maximum Activation of Convolutions (R-MAC) [30] right before the average pool layer, aggregated over three input scales (512,  $512/\sqrt{2}$ , 256) to obtain the representations for learning a metric. For our AGML method, we set  $\gamma = 0.99$  in (3),  $k = 50$  in (2),  $\alpha = 45^\circ$  in (5), and embedding size of 128. We run for a maximum of 100 epochs and choose the best model. We choose 5 labeled examples per class. We easily outperform the baselines by using extremely few labeled examples (see Table 2). This shows the promise of our method. Further ablation studies can be found in the supplementary.

Figures 5 and 6 show top four retrieved images for a query image as obtained by our AGML method and the recently proposed state-of-the-art ISDML approach respectively (please see supplementary for the other methods). For a query image, a red box around a retrieved image denotes an incorrect retrieval, while a green box around a retrieved image denotes a correct retrieval. As observed, the retrieval results of our method are superior to those of the baseline.

## 7 Conclusion

In this paper, we proposed a semi-supervised metric learning approach to reduce the dependency of metric learning on labeled examples. By making use of a nearest neighbor graph, we performed affinity propagation from labeled pairs of data to the unlabeled ones. We inspected the affinities among examples in the neighborhood of an anchor, to form triplets. By using the triplets, we proposed a stochastic approach for metric learning. Additionally, to avoid a degenerate solution, we impose geometric constraints on the parametric matrix of the embedding. This is done by learning an orthogonal matrix within the loss layer without disturbing the backpropagation for SGD. We demonstrated the effectiveness of our method on a number of benchmark datasets by comparing it against baseline semi-supervised metric learning methods.

## References

- [1] Steven C.H. Hoi, Wei Liu, and Shih-Fu Chang. Semi-supervised distance metric learning for collaborative image retrieval and clustering. *ACM Transactions on Multimedia Computing, Communications, and Applications*



Figure 5: Retrieval results in Cars-196 dataset [27] for our AGML method.

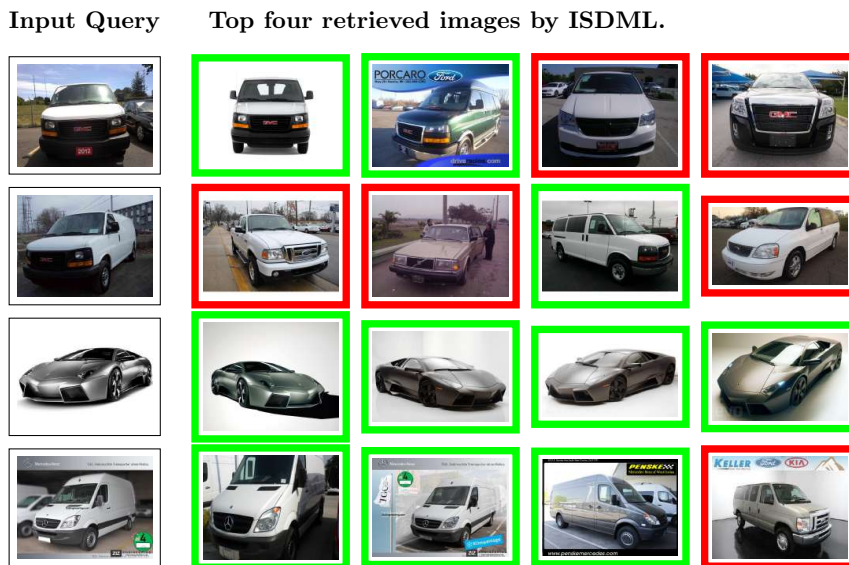


Figure 6: Retrieval results in Cars-196 dataset [27] for the ISDML method.

(*TOMM*), 6(3):18, 2010. 1, 6, 7

- [2] Xiaofei He and Partha Niyogi. Locality preserving projections. In *Proc. of Neural Information Processing Systems (NeurIPS)*, pages 153–160, 2003. 1
- [3] Ujjal Kr Dutta and C Chandra Sekhar. Affinity propagation based closed-form semi-supervised metric learning framework. In *Proc. of International Conference on Artificial Neural Networks (ICANN)*, pages 556–565. Springer, 2018. 2, 6, 7
- [4] Shihui Ying, Zhijie Wen, Jun Shi, Yaxin Peng, Jigen Peng, and Hong Qiao. Manifold preserving: An intrinsic approach for semisupervised distance metric learning. *IEEE Transactions on Neural Networks and Learning Systems (TNNLS)*, 29(7):2731–2742, 2017. 2, 6, 7
- [5] Gang Niu, Bo Dai, Makoto Yamada, and Masashi Sugiyama. Information-theoretic semi-supervised metric learning via entropy regularization. *Neural computation*, 26(8):1717–1762, 2014. 2, 6, 7
- [6] Yves Grandvalet and Yoshua Bengio. Semi-supervised learning by entropy minimization. In *Proc. of Neural Information Processing Systems (NeurIPS)*, pages 529–536, 2005. 2



- [7] Dengyong Zhou, Olivier Bousquet, Thomas N Lal, Jason Weston, and Bernhard Schölkopf. Learning with local and global consistency. In *Proc. of Neural Information Processing Systems (NeurIPS)*, pages 321–328, 2004. [2](#)
- [8] Wei Liu, Shiqian Ma, Dacheng Tao, Jianzhuang Liu, and Peng Liu. Semi-supervised sparse metric learning using alternating linearization optimization. In *Proc. of ACM International Conference on Special Interest Group on Knowledge Discovery and Data Mining (SIGKDD)*, pages 1139–1148, 2010. [2](#), [4](#), [7](#)
- [9] Hyun Oh Song, Yu Xiang, Stefanie Jegelka, and Silvio Savarese. Deep metric learning via lifted structured feature embedding. In *Proc. of IEEE Conference on Computer Vision and Pattern Recognition (CVPR)*, pages 4004–4012, 2016. [3](#), [7](#)
- [10] Jian Wang, Feng Zhou, Shilei Wen, Xiao Liu, and Yuanqing Lin. Deep metric learning with angular loss. In *Proc. of IEEE International Conference on Computer Vision (ICCV)*, 2017. [3](#), [5](#), [6](#)
- [11] Pengtao Xie, Wei Wu, Yichen Zhu, and Eric P Xing. Orthogonality-promoting distance metric learning: convex relaxation and theoretical analysis. In *Proc. of International Conference on Machine Learning (ICML)*, 2018. [3](#)
- [12] Florian Schroff, Dmitry Kalenichenko, and James Philbin. Facenet: A unified embedding for face recognition and clustering. In *Proc. of IEEE Conference on Computer Vision and Pattern Recognition (CVPR)*, pages 815–823, 2015. [3](#)
- [13] Soumava Kumar Roy, Mehrtash Harandi, Richard Nock, and Richard Hartley. Siamese networks: The tale of two manifolds. In *Proc. of IEEE International Conference on Computer Vision (ICCV)*, pages 3046–3055, 2019. [3](#)
- [14] Nitin Bansal, Xiaohan Chen, and Zhangyang Wang. Can we gain more from orthogonality regularizations in training deep networks? In *Proc. of Neural Information Processing Systems (NeurIPS)*, pages 4261–4271, 2018. [3](#)
- [15] Li Jing, Yichen Shen, Tena Dubcek, John Peurifoy, Scott Skirlo, Yann LeCun, Max Tegmark, and Marin Soljačić. Tunable efficient unitary neural networks (eunn) and their application to rnns. In *Proc. of International Conference on Machine Learning (ICML)*, pages 1733–1741, 2017. [3](#)
- [16] Yong Chen, Hui Zhang, Yongxin Tong, and Ming Lu. Diversity regularized latent semantic match for hashing. *Neurocomputing*, 230:77–87, 2017. [3](#)
- [17] Ramin Raziperchikolaei and Miguel A Carreira-Perpinán. Learning independent, diverse binary hash functions: Pruning and locality. In *Proc. of International Conference on Data Mining (ICDM)*, pages 1173–1178. IEEE, 2016. [3](#)
- [18] Daixin Wang, Peng Cui, Mingdong Ou, and Wenwu Zhu. Deep multimodal hashing with orthogonal regularization. In *Proc. of International Joint Conference on Artificial Intelligence (IJCAI)*, 2015. [3](#)
- [19] Pengtao Xie. Learning compact and effective distance metrics with diversity regularization. In *Proc. of European Conference on Machine Learning (ECML)*, pages 610–624. Springer, 2015. [3](#)
- [20] Soumava Kumar Roy, Zakaria Mhammedi, and Mehrtash Harandi. Geometry aware constrained optimization techniques for deep learning. In *Proc. of IEEE Conference on Computer Vision and Pattern Recognition (CVPR)*, pages 4460–4469, 2018. [3](#)
- [21] P-A Absil, Robert Mahony, and Rodolphe Sepulchre. *Optimization algorithms on matrix manifolds*. Princeton University Press, 2009. [3](#)
- [22] Yann LeCun, Léon Bottou, Yoshua Bengio, and Patrick Haffner. Gradient-based learning applied to document recognition. *Proceedings of the IEEE*, 86(11):2278–2324, 1998. [6](#)
- [23] Han Xiao, Kashif Rasul, and Roland Vollgraf. Fashion-mnist: a novel image dataset for benchmarking machine learning algorithms. *arXiv preprint arXiv:1708.07747*, 2017. [6](#)
- [24] Alex Krizhevsky, Geoffrey Hinton, et al. Learning multiple layers of features from tiny images. Technical report, Citeseer, 2009. [6](#)
- [25] Andrea Vedaldi and Karel Lenc. Matconvnet: Convolutional neural networks for matlab. In *Proceedings of the 23rd ACM international conference on Multimedia*, pages 689–692. ACM, 2015. [6](#), [7](#)
- [26] P. Welinder, S. Branson, T. Mita, C. Wah, F. Schroff, S. Belongie, and P. Perona. Caltech-UCSD Birds 200. Technical Report CNS-TR-2010-001, California Institute of Technology, 2010. [7](#)
- [27] Jonathan Krause, Michael Stark, Jia Deng, and Li Fei-Fei. 3d object representations for fine-grained categorization. In *Proc. of IEEE International Conference on Computer Vision Workshops (ICCVW)*, pages 554–561, 2013. [7](#), [8](#)
- [28] Christian Szegedy, Wei Liu, Yangqing Jia, Pierre Sermanet, Scott Reed, Dragomir Anguelov, Dumitru Erhan, Vincent Vanhoucke, and Andrew Rabinovich. Going deeper with convolutions. In *Proc. of IEEE Conference on Computer Vision and Pattern Recognition (CVPR)*, pages 1–9, 2015. [7](#)

- [29] Olga Russakovsky, Jia Deng, Hao Su, Jonathan Krause, Sanjeev Satheesh, Sean Ma, Zhiheng Huang, Andrej Karpathy, Aditya Khosla, Michael Bernstein, et al. Imagenet large scale visual recognition challenge. *International journal of computer vision (IJCV)*, 115(3):211–252, 2015. 7
- [30] Giorgos Tolias, Ronan Sifre, and Hervé Jégou. Particular object retrieval with integral max-pooling of cnn activations. In *Proc. of International Conference on Learning Representations (ICLR)*, 2016. 7